

Nuclear physics method to detect size, timespan and flow in nanoplasmonic fusion

L.P. Csernai^{1,2,3,4}, T. Csörgő,¹ I. Papp^{1,6}, M. Csete^{1,5}, András Szenes^{1,5}, Dávid Vass^{1,5}, T.S. Biró¹ and N. Kroó¹

(part of NAPLIFE Collaboration)

¹ *HUN-REN Wigner Research Centre for Physics, Budapest, Hungary*

² *Department of Physics and Technology, University of Bergen, Norway*

³ *Frankfurt Institute for Advanced Studies, Frankfurt am Main, Germany*

⁴ *Csernai Consult Bergen, Bergen, Norway*

⁵ *Department of Optics and Quantum Electronics, University of Szeged, Szeged, Hungary.*

⁶ *HUN-REN Centre for Energy Research, Budapest, Hungary*

(Dated: November 30, 2023)

The differential Hanbury-Brown and Twiss analysis is widely used in astrophysics and in relativistic heavy ion physics to determine the size and timespan of emitted particles. Here we propose to adopt this method for laser induced nanoplasmonic inertial confinement fusion. The aim is to determine the parameters of emitted Deuterium and Helium⁴ nuclei at the ignition of the fusion target. In addition of spatial volume and timespan the method is able to detect specific space-time correlation patterns, which are connected to collective flow at ignition.

I. INTRODUCTION

The Hanbury Brown and Twiss (HBT) analysis, stemming from astrophysics is a combination of standard two particle correlation functions; it is adequate to analyze the size, timespan, of hadronization in relativistic heavy ion collisions [1] and even collective flow [2, 3] It is based on the Boson's wave function properties.

Laser induced nanoplasmonic fusion reactions even at very low laser pulse energy of 30 mJ showed the creation of deuterium atoms and even He⁴ atoms in small quantities(?). The nuclei of these particles are bosons [4–7]. These bosons with the same quantum structure are expected to show the same correlation properties as the emitted particles at high energies.

Proton and heavier ion acceleration by intensive laser beam is well studied by the ponderomotive force and by the Target Normal Sheath Acceleration (TNSA). Using these techniques even medical cancer treatment was envisaged for quite some time. Recently the unique method was propose to apply resonant plasmonic nanorod antennas for the regulation of local absorption of the laser beam energy and momentum. This method by the NAPLIFE collaboration [8] opened new possibilities. With two sided irradiation in one dimensional geometry it will ensure rapid, stable ignition avoiding the Rayleigh-Taylor instability [9]. Using the Laser Wake Field Acceleration (LWFA) large number of electrons as plasmonic excitation may attract collectively protons (or other ions) to large energies. Furthermore, in the two colliding laser beam wake field collider (LWFC) configuration [10], the emitted protons are dominantly directed in the direction of the Electric field of the laser beam, (which is linearly polarized). For this we need the LWFC configuration and the LWFA mechanism for the proton (or ion) acceleration. The direction of the Electric field is orthogonal to the detection of the laser irradiation.

The plasmonic nano-rod antennas serve as resonant accelerator modules, which accelerate neighbouring protons (or ions) with the LWFA mechanism, Fig. 1. The one-

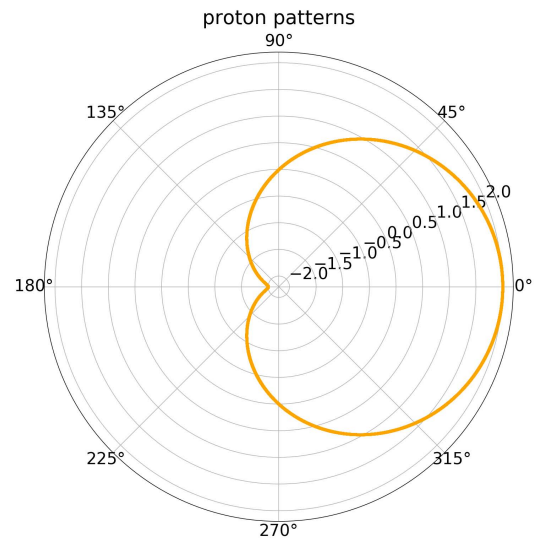


FIG. 1. The angular distribution, of emitted protons along a nanorod antenna irradiated in the LWFA configuration with a step function, from **one** side only in the $z = 0^\circ$ direction with a 30mJ laser pulse with constant intensity, $I = 4 \cdot 10^{17}$ W/cm² in the rest frame of the antenna. The distribution is shown $t = 42.46$ fs after the start of the irradiation. In this case the protons show the beam directed momentum of the laser field irradiation. The antenna and the \mathbf{E} field of the laser beam point in the orthogonal, $x = 90^\circ$ direction. The contours are exponential in arbitrary units.

sided irradiation from the left to the right, i.e. in the z -direction transfers considerable amount of momentum to the protons and electrons, which is clearly shown in the $\pm z$ asymmetry of the distribution.

If in the LWFC configuration, irradiate the nanoantenna from both sides, $z = 0^\circ/180^\circ$, so that the beams constructively interfere in the middle of the reference frame, where the nanorod antenna is positioned, the transferred z -directed momentum is annulled, while the standing waves in this configuration result in vertical

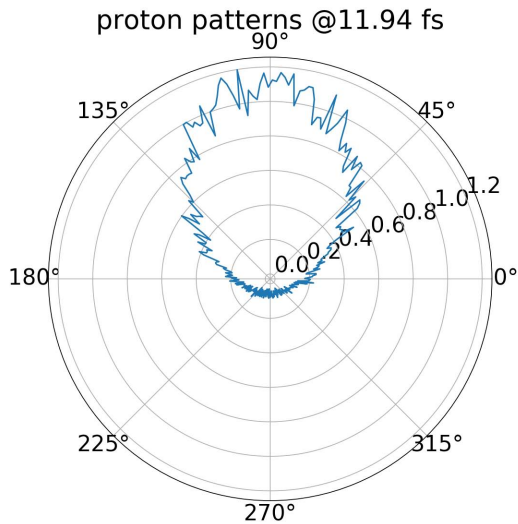


FIG. 2. The angular distribution, of emitted protons along a nanorod antenna irradiated from **two** sides in the LWFA configuration, in the $z = 0^\circ/180^\circ$ direction with a 30mJ laser pulse with constant intensity, $I = 4 \cdot 10^{17}$ W/cm², with a step function profile in the rest frame of the antenna. The distribution is shown one time period T_P after the initial transients, t_o , i.e. at $t_o + T_P = 11.94$ fs after the start of the irradiation. The antenna and the \mathbf{E} field of the laser beam point into the $x = 90^\circ$ direction. The outermost contour (1.0 MeV/c) belongs to momentum of all protons emitted into a solid angle domain of $4\pi/300$. The momentum of the most energetic protons is 13 keV/c. The number of proton marker particles in the EPOCH generated sample is 337058.

electron and proton acceleration i.e. in $\pm x = 90^\circ/270^\circ$ directions, Figs. 2-4. The time period of the irradiating laser beam is $T_P = 2.65$ fs, which corresponds to $\lambda = 800$ nm in vacuum. The total irradiation time for the beam to cross a target of $21 \mu\text{m}$ is about 106 fs. we assume that the intensity of irradiation is constant in this time.

After the start of the irradiation the electrons start to resonantly move in the nano-antenna and the protons around the antenna follow in the LWFC configuration. after an initial transient period of $t_o = 9.3$ fs the proton resonance sets in also and this becomes noticeable after a couple of time periods, T_P , Fig. 2. While in the initial few periods the proton energies slowly increase by $t = 18.5$ fs these reach $p = 1$ MeV/c, by $t = 19.8$ fs these reach $p = 1.7$ MeV/c, and by $t = 106$ fs these reach $p = 12.2$ MeV/c.

This proton acceleration is achieved by the collective plasmonic excitation of very large number of correlated electrons. At the same time the total energy of the accelerated protons increases much stronger, and by 100 fs it reaches 10 GeV/c, in a small solid angle range.

At the same time the energy of the electromagnetic field in the Calculation Box surrounding the nanorod antenna decreases by 20-30 % in 106 fs (see Fig. 3 in ref. [11]), both in the EPOCH and in the COMSOL model evaluations. This drives the electron plasmonic resonant wave as well as the proton resonance and acceleration.

Longer irradiation times increase the amount of protons in the same solid angle domain, which becomes increasingly narrower. At 100 fs the proton momentum in the given solid angle domain of $4\pi/300$ reaches 10 GeV/c, mainly due to the increased number of protons in this domain. The shape becomes rather narrow in the $\pm x$ axis peaking in both directions.

We present and analyse this method and its results in a high resolution, Particle In Cell EPOCH kinetic model, similarly as it is done for PICR fluid dynamics [2, 3]. Fluid dynamics is proven to be the best theoretical method to describe collective flow phenomena. The same model was used to predict the rotation in peripheral ultra-relativistic reactions [12], to point out the possibility of Kelvin Helmholtz Instability (KHI) [13], flow vorticity [14] and polarization arising from local rotation, i.e. vorticity [15]. The model was also tested for its numerical viscosity and the resulting entropy production [16].

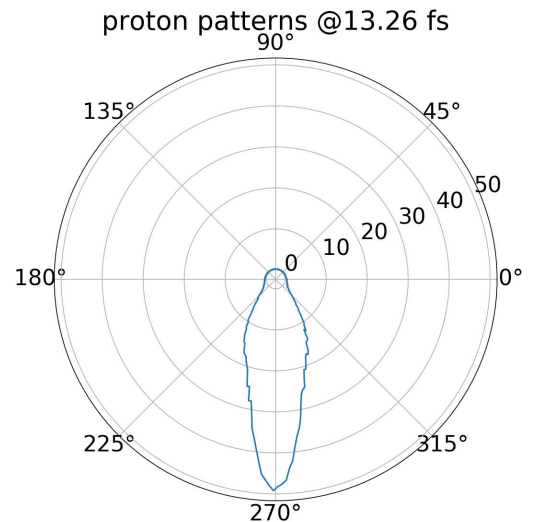


FIG. 3. The same as Fig. 2 for $t_o + 1.5T_P = 13.26$ fs after the start of the irradiation, i.e. half period later. The direction of the motion of protons is reversed just as the electric field. The outermost contour (50 MeV/c) belongs to momentum of all protons emitted into a solid angle domain of $4\pi/300$. The momentum of the most energetic protons is 36 keV/c, more than earlier in Fig. 2, but the increase of the total momentum in the domain is due to the increased number of the resonating protons.

The two particle correlation studies are used in the field of ultra-relativistic heavy ion physics for a long time and these studies were developed to a high level of sophistication determining not only size and timespan of an emitting source, but its shape, its dynamics, its expansion and rotation. At CERN the high resolution event by event 4π detectors provided a massive amount of data for two particle correlation studies. In present, limited budget laser fusion studies such detector systems are not always affordable, but one or two detectors are available.

Just as in astrophysics these smaller detector accep-

tances may provide sufficient data for important and essential consequences [17, 18].

II. CORRELATION FUNCTION

The boson correlation function is defined as the inclusive two-particle distribution divided by the product of the inclusive one-particle distributions, such that [1]:

$$C(p_1, p_2) = \frac{P_2(p_1, p_2)}{P_1(p_1)P_1(p_2)}, \quad (1)$$

where p_1 and p_2 are the 4-momenta of particles.

In order to be able to measure such a correlation function we need a detector (or more), which is able to detect at least two simultaneous bosons emitted directly from the fusion ignition, where these were created. These particles should not have other interactions or collisions (or should not recombine to form atoms or molecules) before detection.

We introduce the center-of-mass momentum ¹: $k = \frac{1}{2}(p_1 + p_2)$, and the relative momentum $q = p_1 - p_2$, where from the mass-shell condition [1] $q^0 = \mathbf{k}\mathbf{q}/k^0$. We use a method for moving sources presented in Ref. [19].

$$C(k, q) = 1 + \frac{R(k, q)}{|\int d^4x S(x, k)|^2}, \quad (2)$$

where²

$$R(k, q) = \int d^4x_1 d^4x_2 \cos[q(x_1 - x_2)] \times S(x_1, k + q/2) S(x_2, k - q/2). \quad (3)$$

Using the emission function $S(x, k)$, discussed in ref. [24], here $R(k, q)$ can be calculated [19, 20, 22?] via the function

$$J(k, q) = \int d^4x S(x, k + q/2) \exp(iqx), \quad (4)$$

and we obtain the $R(k, q)$ function as $R(k, q) = \text{Re}[J(k, q)J(k, -q)]$.

We estimate the local particle (boson) density $n(x)$ based on the EPOCH kinetic model using the PIC method. ²

For now we will use the equilibrium single particle distribution, $f^J(x, p)$, in the source functions, i.e. the

Jüttner distribution, which depends on the local velocity, $u^\mu(x)$, and we use the notation $u_1 = u(x_1) = u^\mu(x_1)$ and temperature T .

$$f^J(x, p) = \frac{n(x)}{C_\pi (2\pi\hbar)^3} \exp\left(\frac{-p^\mu u_\mu(x)}{T(x)}\right), \quad (5)$$

where $C_\pi = 4\pi m_B^2 T K_2(m_B/T)$, at temperature T , and K_2 is a modified Bessel function and m_B is the boson mass.

The Cancelling Jüttner (CJ) distribution, f_{CJ} , is defined by subtracting the ordinary Jüttner distribution (5) with negative velocity, $-v$, from original Jüttner distribution, and multiplying the obtained result with the step function (Fig. 5):

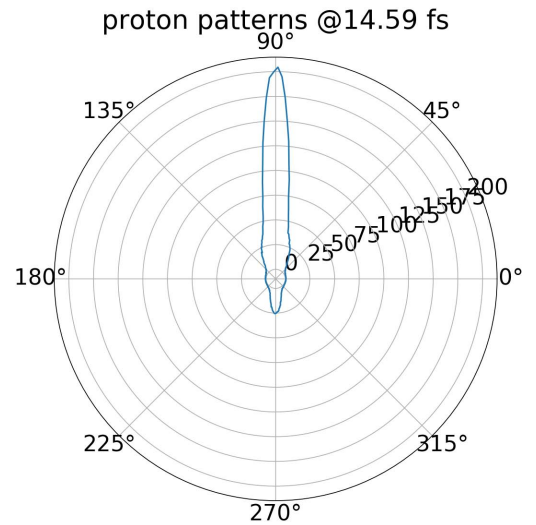


FIG. 4. The same as Figs. 2 and 3 for $t_o + 2T_P = 14.59$ fs after the start of the irradiation, i.e. another half period later. The direction of the motion of protons is reversed again. The outermost contour (200 MeV/c) belongs to momentum of all protons emitted into the same solid angle domain. The energy of the most energetic protons is 68 keV/c, more than before in Fig. 3, but the increase of the total momentum in the domain is due to the increased number of the resonating protons. The angular spread of the distribution becomes narrower at the same time.

Thus the local invariant particle density is given by the Cancelling Jüttner (CJ) distribution [23]:

$$f_{CJ} = \frac{\Theta(p^\mu d\sigma_\mu) n(x)}{C_\pi (2\pi\hbar)^3} \times \left(\exp\left(\frac{-p^\mu u_\mu^R}{T}\right) - \exp\left(\frac{-p^\mu u_\mu^L}{T}\right) \right), \quad (6)$$

where $d\sigma_\mu$ for a single nanorod is the unit normal vector pointing in the direction of the nanorod antenna. In case of a full scale macroscopic modeling $d\sigma_\mu$ points to the direction of the momentum of the marker particle m_d or m_{He^4} . Here $u_\mu^R = (\gamma, \gamma v, 0, 0)$ and $u_\mu^L = (\gamma, -\gamma v, 0, 0)$ in the rest frame of the nanorod or the marker particle.

¹ The vector \mathbf{k} is the wavenumber vector, $\mathbf{k} = \mathbf{p}/\hbar$ so for numerical calculations we have to use that $\hbar c = 197.327$ MeV fm., The same applies to \mathbf{q} .

² The net boson density is sufficiently large in macroscopic experiments, so this approximation is satisfactory. At the present time the detection of bosons is relatively limited, so the adequate measurement technique should still be worked out².

When $p^\mu d\sigma_\mu = 0$ the function vanishes at the front, even without step function Θ . The role of the $\Theta(p^\mu d\sigma_\mu)$ part is just to eliminate the negative part of the distribution.

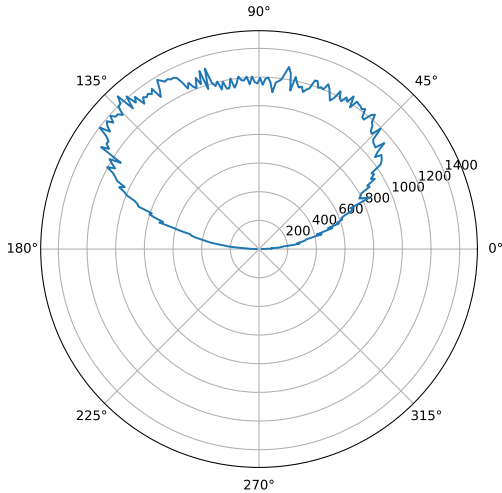


FIG. 5. Polar histogram of the Cancelling Jüttner (CJ) distribution for a generated random sample of 300000 protons averaged in 200 bins. The results in similar pattern as observed in the simulation. The CJ distribution is shifted by $v = 0.7c$. The distribution resembles the EPOCH generated distribution shown in Fig. 2.

The CJ distribution II resembles strongly the distribution obtained in the EPOCH kinetic theory, Figs. 2 (and 3). The increasingly narrower distributions can be simulated with increasing velocities v . The "temperature" parameter T in our case is representing the random spread of the kinetic distribution, and this is decreasing rapidly. In case of Fig. 2, $T \sim 13$ keV, similar to the max proton energy. In case of Fig. 3, $T \sim 10$ keV approximately one third of the max proton energy.

In case of extreme narrow distributions at late times as 100 fs, single velocity, non-equilibrated distributions can be used instead of the Cancelling Jüttner distributions in the two particle correlation studies.

If we assume that the two coincident particles originate from two points, x_1 and x_2 , the expression of the correlation function, Eq. (3) will be become [24]

$$R(k, q) = \int d^4x_1 d^4x_2 S(x_1, k) S(x_2, k) \cos[q(x_1 - x_2)] \times \exp\left[-\frac{q}{2} \cdot \left(\frac{u(x_1)}{T(x_1)} - \frac{u(x_2)}{T(x_2)}\right)\right], \quad (7)$$

and the corresponding $J(k, q)$ -function is

$$J(k, q) = \int d^4x S(x, k) \exp\left[-\frac{q \cdot u(x)}{2T(x)}\right] \exp(iqx), \quad (8)$$

In Ref. [24] different one, two and four source systems were tested with and without rotation. Here we study only the case where the emission is *asymmetric* and dominated by the fluid elements facing the detector.

The modeling for laser induced fusion can be made in two steps. First we model one nanorod. In this case the emission is in the direction of the nanorod, which is orthogonal to the laser irradiation and points into the direction of polarization of laser light. Electrons and protons are accelerated in this direction, and consequently also the deuterium and He^4 particles will have a main direction of emission in this direction. For this stage this will be the symmetry axis ($d\sigma^\mu$) pointing in the z direction. The obtained spread of the distribution can be fitted to the velocity, v and "temperature", T parameter of the CJ distribution.

In the second macroscopic step we can identify the marker particles. these will be our elements of source, s , and their direction of motion will be our symmetry axis, z , for the macroscopic step.

Let us consider the usual conventions, z is the irradiation beam axis, and the positive z -direction is the direction of the laser beam. The laser's polarization vector points into the positive x -direction. Finally the y -axis is orthogonal to both. The emission probabilities from the two source cells of a pair are generally not equal.

The laser induced fusion in a one dimensional LWFC collaboration needs a target of $20 \mu\text{m}$ thick target with a beam diameter of about $10\text{-}30 \mu\text{m}$. This is certainly a macroscopic size target compared to an Event by Event relativistic heavy ion collision. Thus we will attack the problem in two steps: first we analyze the correlation function for one nanorod in the EPOCH kinetic PIC model, and then as a second step we treat the problem in a fluid dynamical type approach, while keeping the non-equilibrium and non-thermal features in the analysis.

III. ONE FLUID CELL AS SOURCE

We now assume a source function, which is reduced to one ignition time moment. Thus the integration over the 4-volume of an emission layer is reduced to the 3-volume of a FO hyper surface. For simplicity of this presentation, we assume emission along the time like coordinate, t , where we assume a local Jüttner distribution. Thus, we have the source function as

$$S(x, k) = G(x) H(t) \exp\left(-\frac{k_\mu u^\mu(x)}{T(x)}\right) k^\mu \hat{\sigma}_\mu, \quad (9)$$

where $k^\mu \hat{\sigma}_\mu$ is an invariant scalar, and $\hat{\sigma}_\mu$ is a unit vector pointing in the axis, x -direction, of the nanorod antenna. This is the same as the \mathbf{E} field or polarization direction of the laser beam. Furthermore for the simplicity of presentation we assume Jüttner distribution instead of Cancelling Jüttner, and a "temperature" T and velocity v . Later these can be replaced by the fitted Cancelling

Jüttner parameters and the energy density of the spread of particle emission distribution.

For simple presentation take a single cell and let us use a simple quadratic parametrization for $n(x)$ as:

$$G(x) = \gamma n(x) = \gamma n_s \exp\left(-\frac{x^2 + y^2 + z^2}{2R^2}\right). \quad (10)$$

Here n_s is the average density of the Gaussian source (or fluid cell) of mean radius R .

Single source at rest: The invariant scalar $k^\mu u_\mu$ can be calculated in the frame where the cell is at rest. We have then

$$u^\mu = (1, 0, 0, 0) \Rightarrow -\frac{k_\mu u^\mu}{T} = -\frac{k^0}{T} = -\frac{E_k}{T}. \quad (11)$$

In this simplest case we also assume that the FO direction is $\hat{\sigma}^\mu = (1, 0, 0, 0)$, so the τ -coordinate coincides with the t -coordinate, and it is orthogonal to the x, y, z coordinates. Then we can make use of the following integral:

$$\int_{-\infty}^{+\infty} e^{-ax^2} d^3x = \left(\frac{\sqrt{\pi}}{\sqrt{a}}\right)^3. \quad (12)$$

We can perform the integral along the t direction of $H(t)$, which gives unity and then the single particle distribution is

$$\begin{aligned} \int d^4x S(x, k) &= \frac{n_s(k^\mu \hat{\sigma}_\mu)}{C_n} \exp\left(-\frac{E_k}{T_s}\right) \times \\ \int_{-\infty}^{+\infty} H(t) dt \int_{-\infty}^{+\infty} e^{-\frac{x^2}{2R^2}} dx \int_{-\infty}^{+\infty} e^{-\frac{y^2}{2R^2}} dy \int_{-\infty}^{+\infty} e^{-\frac{z^2}{2R^2}} dz &= \\ n_s(k^\mu \hat{\sigma}_\mu) \exp\left(-\frac{E_k}{T_s}\right) \frac{(2\pi R^2)^{3/2}}{C_n}, \end{aligned} \quad (13)$$

here T_s is the "temperature" of the source, and $E_k = k^0$ in the rest frame of the fluid cell. Due to the normalization of $H(t)$ the integral over the time t is unity. The contribution to the nominator from Eq. (8) is

$$\begin{aligned} J(k, q) &= \int d^4x e^{iq \cdot x} e^{-q^0/(2T_s)} S(x, k) = \\ &= \frac{n_s(k^\mu \hat{\sigma}_\mu)}{C_n} \exp\left[-\frac{E_k + q^0/2}{T_s}\right] \times \\ &= \int_{-\infty}^{+\infty} H(t) e^{iq^0 t} dt \int_{-\infty}^{+\infty} e^{-\frac{x^2}{2R^2}} e^{-iq_x x} dx \times \\ &= \int_{-\infty}^{+\infty} e^{-\frac{y^2}{2R^2}} e^{-iq_y y} dy \int_{-\infty}^{+\infty} e^{-\frac{z^2}{2R^2}} e^{-iq_z z} dz = \\ &= \frac{n_s(k^\mu \hat{\sigma}_\mu)}{C_n} (2\pi R^2)^{3/2} \exp\left[-\frac{E_k}{T_s}\right] \exp\left[-\frac{q^0}{2T_s}\right] \times \\ &= \exp\left[-\frac{R^2}{2} q^2\right] \exp\left[-\frac{\Theta^2}{2} (\hat{\sigma}^\mu q_\mu)^2\right], \end{aligned} \quad (14)$$

where we used $\int_{-\infty}^{+\infty} \exp(-p^2 x^2 \pm qx) dx = (\sqrt{\pi}/p) \times \exp(q^2/(4p^2))$ [25]:3.323/2. In the time integral the present choice of $\hat{\sigma}^\mu$ would give $(q^0)^2$, but we wanted to indicate that other choices are also possible and they would yield $(\hat{\sigma}^\mu q_\mu)^2$. In the $J(k, q)J(k, -q)$ product the terms $\exp[\pm q^0/(2T_s)]$ cancel each other.

These integrals can be performed for the Canceling Jüttner and for the non-thermal constant velocity distributions also.

Inserting these equations into (2) we get

$$C(k, q) = 1 + \exp\left(-(\Delta\tau)^2 (\hat{\sigma}^\mu q_\mu)^2 - R^2 q^2\right). \quad (15)$$

If we have a source point, which is at longer distance from the external side of the source Θ , then the contribution of the time integral from this point is reduced.

If we tend to an infinitely narrow source layer, "sudden full ignition", $\Theta \rightarrow 0$, i.e. to a source hyper-surface, then

$$C(k, q) = 1 + \exp\left(-R^2 q^2\right). \quad (16)$$

The k dependence drops out from the correlation function, C as the k dependent parts are separable, Fig. 6.

In our EPOCH PIC studies modeling a single nano-rod antenna and its surrounding we counted and analyzed a Calculation Box of $530 \times 530 \times 795$ nm. Thus a typical radius of such a system is slightly under $1 \mu\text{m}$.

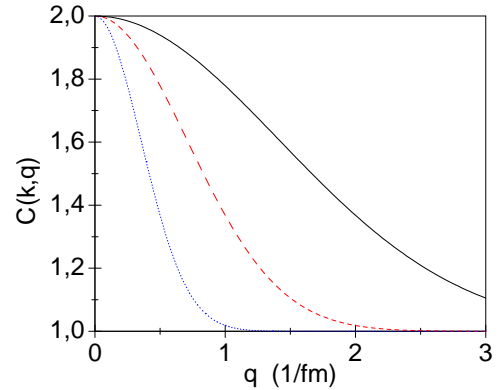


FIG. 6. (color online) The correlation function, $C(k, q)$, for a single, static, spherically symmetric, Gaussian source with different radii, $R = 4, 1$ and $0.25 \mu\text{m}$, (blue dotted, red dashed, and full black lines respectively), as described by Eq. (16).

In case of more involved time dependence of the source the correlation function becomes also more complex, which needs adequate analysis.

For the study of the rotation of the system the thickness of the 4D ignition layer is of secondary importance, especially if we discuss only a few fluid source cells. In this case the role of the depth of a source point within the layer is given by its reduced contribution to the particle emission. This can be represented much simpler with assigning emission weights to the small number of sources. Thus, in the following discussion, we do not go into the details of the time structure of the emission.

IV. OUTLOOK

The two particle correlation measurements for laser induced nanoplasmonic inertial confinement fusion can be used in two stages. At relatively small laser beam energy pulses from 30 mJ energy one can see already nuclear reactions, deuterium production. This is due to the increased proton energy caused by the catalysing effect of nanorod antennas. Up to now the volume and time extent of the "Irradiation Volume" was only theoretically estimated [7]. Recent theoretical analysis indicates that nanorod antennas may catalyse proton acceleration [26], which enables nuclear transmutation and thus fusion reactions.

Two particle correlation analysis with even one or two particle detectors only can provide experimental measure for this intermediate source object dynamically. Up to now only the crater volume was measured caused by these nuclear transmutation reactions in the target.

In the future with increased beam intensity and laser pulse energy at ELI-ALPS we expect energy producing exothermic ^4He production, the volume and time extent of the formation domain are vital for further development of the technology based on nanoplasmonics assisted laser

induced fusion.

In case of fusion target with oriented nanorods the angular distribution of proton emission can be verified, which confirms experimentally the directed proton acceleration mechanism by the applied nanorod catalyzed fusion method.

Acknowledgements: L. P. Csernai acknowledges support from Wigner Research Center for Physics, Budapest (2022-2.2.1-NL-2022-00002). T.S. Biró, M. Csete, N. Kroó, I. Papp, acknowledges support by the National Research, Development and Innovation Office (NKFIH) of Hungary. We would like to thank the Wigner GPU Laboratory at the Wigner Research Center for Physics for providing support in computational resources. This work is supported in part by the Frankfurt Institute for Advanced Studies, Germany, the Hungarian Research Network, the Research Council of Norway, grant no. 255253, and the National Research, Development and Innovation Office of Hungary, for projects: Nanoplasmonic Laser Fusion Research Laboratory under project numbers NKFIH-874-2/2020 and NKFIH-468-3/2021, Optimized nanoplasmonics (K116362), and Ultrafast physical processes in atoms, molecules, nanostructures and biological systems (EFOP-3.6.2-16-2017-00005).

-
- [1] W. Florkowski: *Phenomenology of Ultra-relativistic heavy-Ion Collisions*, World Scientific Publishing Co., Singapore (2010).
- [2] L. P. Csernai and S. Velle, Study of rotating high energy systems with the differential HBT method, *Int. J. of Modern Physics E* **23** (9), 1450043 (2014).
- [3] L. P. Csernai, S. Velle, and D. J. Wang, New method to detect rotation in high-energy heavy-ion collisions *Phys. Rev. C* **89**, 034916 (2014).
- [4] I. Rigó, J. Kámán, Á. Nagyné Szokol, A. Bonyár, M. Szalóki, A. Borók, Shereen Zangana, P. Rácz et al., Márk Aladi, Miklós Ákos Kedves, Gábor Galbács, (NAPLIFE Collaboration) Raman spectroscopic characterization of crater walls formed upon single-shot high energy femtosecond laser irradiation of dimethacrylate polymer doped with plasmonic gold nanorods arXiv: 2210.00619 [physics.plasm-ph],
- [5] Archana Kumari, invited talk - for the NAPLIFE Collaboration: LIBS Analysis of Pure, Deuterated and Au-doped UDMA: TEGDMA mixture: A Part of the Nanoplasmonic Laser Fusion Experiments, 11th Int. Conf. on New Frontiers in Physics 2022, Kolymbari, Crete, Greece, 7th Sept. 2022.
- [6] Péter Rácz, - invited talk - for the NAPLIFE Collaboration, LIBS spectra from polymer shootings,- Margaret Island Symposium 2022 on Vacuum Structure, Particles, and Plasmas, Budapest, May 15-18, 2022.
- [7] László P. Csernai, Igor N. Mishustin, Leonid M. Satarov, Horst Stöcker, Larissa Bravina, Mária Csete, Judit Kám'ann, Archana Kumari, Anton Motornenko, István Papp, Peter Rácz, Daniel D. Strottman, András Szenes, Ágnes Szokol, Dávid Vass, Miklós Veres, Tamás S. Biró, Norbert Kroó (NAPLIFE Collaboration), Crater Formation and Deuterium Production in Laser Irradiation of Polymers with Implanted Nano-antennas, *Phys. Rev. E*, **108**(2) 025205 (2023).
- [8] L. P. Csernai, M. Csete, I. N. Mishustin, A. Motornenko, I. Papp, L. M. Satarov, H. Stöcker, and N. Kroó (NAPLIFE Collaboration), Radiation dominated implosion with flat target, *Physics and Wave Phenomena* **28** 187–199 (2020).
- [9] L.P. Csernai, N. Kroo, and I. Papp, Radiation dominated implosion with nano-plasmonics, *Laser and Particle Beams*, **36** (2), 171-178 (2018).
- [10] István Papp, Larissa Bravina, Mária Csete, Igor N. Mishustin, Dénes Molnár, Anton Motornenko, Leonid M. Satarov, Horst Stöcker, Daniel D. Strottman, András Szenes, Dávid Vass, Tamás S. Biró, László P. Csernai, Norbert Kroó, (NAPLIFE Collaboration), Laser Wake Field Collider; *Phys. Lett. A* **396**, 12724 (2021).
- [11] István Papp, Larissa Bravina, Mária Csete, Archana Kumari, Igor N. Mishustin, Anton Motornenko, Péter Rácz, Leonid M. Satarov, Horst Stöcker, Daniel D. Strottman, András Szenes, Dávid Vass, Ágnes Nagyné Szokol, Judit Kámán, Attila Bonyár, Tamás S. Biró, László P. Csernai, Norbert Kroó (NAPLIFE Collaboration), Kinetic model of resonant nanoantennas in polymer for laser induced fusion, *Front. Phys.* **11**, 1116023 (2023).
- [12] L.P. Csernai, V.K. Magas, H. Stöcker, and D.D. Strottman, Fluid Dynamical Prediction of Changed v1-flow at LHC, *Phys. Rev. C* **84**, 024914 (2011).
- [13] L.P. Csernai, D.D. Strottman and C. Anderlik, Kelvin-Helmholtz instability in high energy heavy ion collisions, *Phys. Rev. C* **85**, 054901 (2012).

- [14] L.P. Csernai, V.K. Magas, and D.J. Wang, Flow Vorticity in Peripheral High Energy Heavy Ion Collisions Phys. Rev. C **87**, 034906 (2013).
- [15] F. Becattini, L.P. Csernai, D.J. Wang, Lambda Polarization in Peripheral Heavy Ion Collisions, Phys. Rev. C **88**, 034905 (2013).
- [16] Sz. Horvát, V.K. Magas, D.D. Strottman, L.P. Csernai, Entropy development in ideal relativistic fluid dynamics with the Bag Model equation of state, Phys. Lett. B **692**, 277 (2010).
- [17] T. Csörgő, B. Lörstad, Bose-Einstein correlations for three-dimensionally expanding, cylindrically symmetric, finite systems Phys. Rev. C **54** (1996) 1390-1403.
- [18] H. Beker, H. Boggild, J. Boissevain, M. Cherney, J. Dodd et al., (CERN-NA44 Collaboration), $m(T)$ dependence of boson interferometry in heavy ion collisions at the CERN SPS, Phys. Rev. Lett. **74** (1995) 3340-3343.
- [19] A.N. Makhlin, Yu.M. Sinyukov, The hydrodynamics of hadron matter under a pion interferometric microscope, Z. Phys. C **39**, 69 (1988).
- [20] S.V. Akkelin, Yu.M. Sinyukov, The HBT-interferometry of expanding inhomogeneous sources Z. Phys. C **72**, 501 (1996).
- [21] T. Csörgő, S.V. Akkelin, Y. Hama, B. Lukács, and Yu.M. Sinyukov, Observables and initial conditions for self-similar ellipsoidal flows, Phys. Rev. C **67**, 034904 (2003).
- [22] T. Csörgő, Particle Interferometry from 40 MeV to 40 TeV, Heavy Ion Phys. **15**, 1-80, (2002).
- [23] K. Tamosiunas and L.P. Csernai, Cancelling Jüttner distributions for space-like freeze-out, Eur. Phys. J. A **20**, 269-275 (2004).
- [24] L.P. Csernai, S. Velle, Differential Hanbury-Brown Twiss method to analyze rotation, arXiv: 1305.0385 (2013).
- [25] I.S. Gradshteyn and I.M. Ryzhik: *Table of integrals, series and products*, Academic Press (1965).
- [26] István Papp, Larissa Bravina, Mária Csete, Archana Kumari, Igor N. Mishustin, Anton Motornenko, Péter Rác, Leonid M. Satarov, Horst Stöcker, András Szenes, Dávid Vass, Tamás S. Biró, László P. Csernai, Norbert Kroó, Laser induced proton acceleration by resonant nano-rod antenna for fusion, arXiv: 2306.13445 [physics.plasm-ph]